Relationship between Measurements of Pollution in the Troposphere (MOPITT) and in situ observations of CO based on a large-scale feature sampled during TRACE-P

J. H. Crawford,[1] C. L. Heald,[2] H. E. Fuelberg,[3] D. M. Morse,[3] G. W. Sachse,[1] L. K. Emmons,[4] J. C. Gille,[4] D. P. Edward,[4] M. N. Deeter,[4] G. Chen,[1] J. R. Olson,[1] V. S. Connors,[1] C. Kittaka,[1] and A. J. Hamlin[1,5]

Received 31 October 2003; revised 20 February 2004; accepted 4 March 2004; published 26 May 2004.

[1] During Transport and Chemical Evolution over the Pacific (TRACE-P), there were several opportunities to perform in situ sampling coincident with overpasses of the Measurements of Pollution in the Troposphere (MOPITT) instrument on board the EOS Terra satellite. This sampling consisted of in situ vertical profiles of CO by NASA's DC-8 aircraft intended to provide data useful for validating MOPITT observations of CO column. One particular profile conducted over the central North Pacific revealed a layer of pollution characterized by CO mixing ratios more than double background values. Sampling of the surrounding region by both the NASA DC-8 and P-3B aircraft showed this layer to have a considerable geographic extent, at least 25° longitude (~2500 km) and 4° latitude (~400 km). Using back trajectory analysis, this polluted layer is followed back in time and compared with four consecutive MOPITT overpasses. MOPITT observations during these four overpasses agree well with the location of the layer as inferred by the trajectories; however, the detected CO column amount increases backward in time by just over 20%. Further analysis shows that the majority of this change in detected column abundance is consistent with two factors: (1) changes in the thickness of the polluted layer over time (9 ± 3%) and (2) changes in retrieved column abundance due to the altitude of the layer (7 ± 3%). This demonstrates that there are both real and artificial sources of variability that must be understood before MOPITT observations can be quantitatively useful. An unexpected finding was the difference in the variance of MOPITT observations depending on whether observations were taken under daylight or nighttime conditions. The variance in daytime observations of the polluted layer was approximately double that for nighttime data. The results of this analysis indicate that targeted in situ sampling of large-scale pollution events can provide insight leading to more realistic interpretation of MOPITT observations. Strategies for sampling such events repeatedly during their evolution could also provide more interesting opportunities for validation. *INDEX TERMS:* 0345 Atmospheric Composition and Structure: Pollution—urban and regional (0305); 0365 Atmospheric Composition and Structure: Troposphere—composition and chemistry; 0368 Atmospheric Composition and Structure: Troposphere—constituent transport and chemistry; 9355 Information Related to Geographic Region: Pacific Ocean; *KEYWORDS:* TRACE-P, MOPITT, carbon monoxide

Citation: Crawford, J. H., et al. (2004), Relationship between Measurements of Pollution in the Troposphere (MOPITT) and in situ observations of CO based on a large-scale feature sampled during TRACE-P, *J. Geophys. Res.*, *109*, D15S04, doi:10.1029/2003JD004308.

1. Introduction

[2] Observations of tropospheric composition are essential to improving our understanding of chemical cycles and their role in the short-term and long-term evolution of the troposphere. Overcoming the paucity of observations continues to be one of the primary challenges to answering key questions about the sources and fates of various chemical species. Historically, in situ observations from aircraft have been the primary means of gathering observations of atmospheric composition throughout the

[1]Atmospheric Sciences, NASA Langley Research Center, Hampton, Virginia, USA.
[2]Department of Earth and Planetary Sciences, Harvard University, Cambridge, Massachusetts, USA.
[3]Department of Meteorology, Florida State University, Tallahassee, Florida, USA.
[4]National Center for Atmospheric Research, Boulder, Colorado, USA.
[5]Now at Department of Engineering Fundamentals, Michigan Technological University, Houghton, Michigan, USA.

0148-0227/04/2003JD004308$09.00

free troposphere and over remote oceanic regions. Measurements from sondes and balloon-borne platforms have also played an important role but have been more limited in the number of species observed. More recently, satellite observations are becoming a significant source of information concerning tropospheric composition [*Singh and Jacob*, 2000]. The promise of much better temporal and spatial resolution from space-based observations, albeit for only a few species, promises to greatly complement airborne observations which are temporally and spatially limited but offer a wealth of detail on composition by the simultaneous measurement of many constituents. It is important then to fully examine the complementary relationship between airborne and satellite observations as opportunities arise.

[3] Spaced-based observations have played a key role in previous airborne missions, most notably NASA's Transport and Atmospheric Chemistry near the Equator-Atlantic (TRACE-A) campaign [*Fishman et al.*, 1996], which deployed to the tropical South Atlantic. The impetus for TRACE-A was the satellite-derived observation of a region of enhanced tropospheric ozone off the west coast of southern Africa during austral spring [*Fishman et al.*, 1990]. NASA's more recent Transport and Chemical Evolution over the Pacific (TRACE-P) campaign [*Jacob et al.*, 2003] presented the first opportunity for a NASA airborne mission focused on tropospheric chemistry to interact directly with a space-based platform. During TRACE-P, NASA's DC-8 aircraft measured in situ vertical profiles of CO coincident with overpasses of Measurements of Pollution in The Troposphere (MOPITT). MOPITT represents one of the first satellite instruments to provide routine measurements of a tropospheric constituent (carbon monoxide, CO) from space. The intent of these in situ CO profiles was to provide data for validation. In addition to in situ measurements in support of MOPITT, global model calculations also have been used to bridge the gap between the aircraft and MOPITT observations of CO from the TRACE-P time period with encouraging results [*Heald et al.*, 2003].

[4] There were seven occasions during TRACE-P when the NASA DC-8 performed validation profiles beneath the MOPITT instrument. Details of these underflights and the resulting data comparisons are discussed by *Jacob et al.* [2003]. One profile conducted during a transit flight over the central Pacific revealed an enhanced layer of pollution with CO mixing ratios more than double background values. Further sampling during transit revealed that this layer possessed a surprising level of homogeneity for CO and other trace species over an extent of $\sim$25° of longitude ($\sim$2500 km) across the central North Pacific.

[5] The following analysis attempts to extend the evaluation of MOPITT beyond the simple validation profile coinciding with the MOPITT overpass. Using back trajectory analysis, the polluted layer is examined as a large regional feature, both at the time of aircraft sampling and back in time through previous satellite overpasses. This offers the opportunity to assess the behavior of the MOPITT observations in a way that is more comprehensive, albeit less rigorous, than that provided by the single point comparison of the validation profile.

2. Instrument Descriptions

2.1. In Situ Measurements

[6] In situ measurements of CO were performed using a folded-path, differential absorption, tunable diode laser spectrometer [*Sachse et al.*, 1987; *Vay et al.*, 1998]. Two versions of the instrument were deployed during TRACE-P: one on NASA's DC-8 aircraft and the other on NASA's P-3B aircraft. Measurements were obtained at a frequency of 1 Hz and a precision of 1 ppbv or 1%. Calibrations were performed on 10 min intervals with measurement accuracy closely tied to the primary calibration standards obtained from the NOAA Climate Monitoring and Diagnostics Laboratory. Intercomparison of the two instruments during close proximity flight of the two aircraft revealed that the instruments agreed within the stated uncertainties [*Eisele et al.*, 2003].

2.2. MOPITT

[7] The MOPITT instrument was launched aboard NASA's EOS Terra satellite in December 1999. This downward viewing instrument uses IR gas correlation radiometry to monitor tropospheric CO and CH_4 [*Drummond and Mand*, 1996] and is capable of making observations during both day and night (CO only). MOPITT's polar Sun-synchronous orbit has an equator crossing time of 1045 LT. The horizontal resolution of MOPITT observations is 22 km $\times$ 22 km with cross-track scanning covering a swath 640 km wide. This cross-track scanning allows for near global coverage in 3 days. CO concentrations are reported for the total column amount and for seven vertical levels (surface, 850, 700, 500, 350, 250, and 150 hPa).

[8] The MOPITT observations used in this analysis are the version 3 retrievals for total CO column (http://www.eos.ucar.edu/mopitt). Details on the MOPITT retrieval algorithm are given by *Deeter et al.* [2003]. Data for individual levels were not used since they offer limited additional information for this study. Specifically, an analysis of MOPITT data for the TRACE-P time period by *Heald et al.* [2003] determined that there are typically fewer than two pieces of independent information per MOPITT pixel over the North Pacific. This is related in part to MOPITT's sensitivity which is minimized at the surface and maximized in the middle troposphere [*Deeter et al.*, 2003]. In order to compare in situ profiles with MOPITT, the vertical resolution and sensitivity of the MOPITT retrievals must be taken into account using the appropriate averaging kernel and a priori profile. In-depth discussion of comparing in situ data to MOPITT and the contribution of TRACE-P data to the broader MOPITT validation effort is given by *Emmons et al.* [2004].

3. Observations of CO for 27 February 2001

[9] On 27 February 2001 both the NASA DC-8 and P-3B aircraft departed from Kona, Hawaii (19°N, 156°W), on transit flights across the central North Pacific. The destinations for the DC-8 and P-3B were Guam (13°N, 145°E) and Wake Island (19°N, 167°E), respectively. During these flights, both aircraft performed extensive atmospheric profiling. In the case of the DC-8, one of the profiles was conducted coincident with an overpass of the MOPITT satellite with the intent of providing data useful for valida-

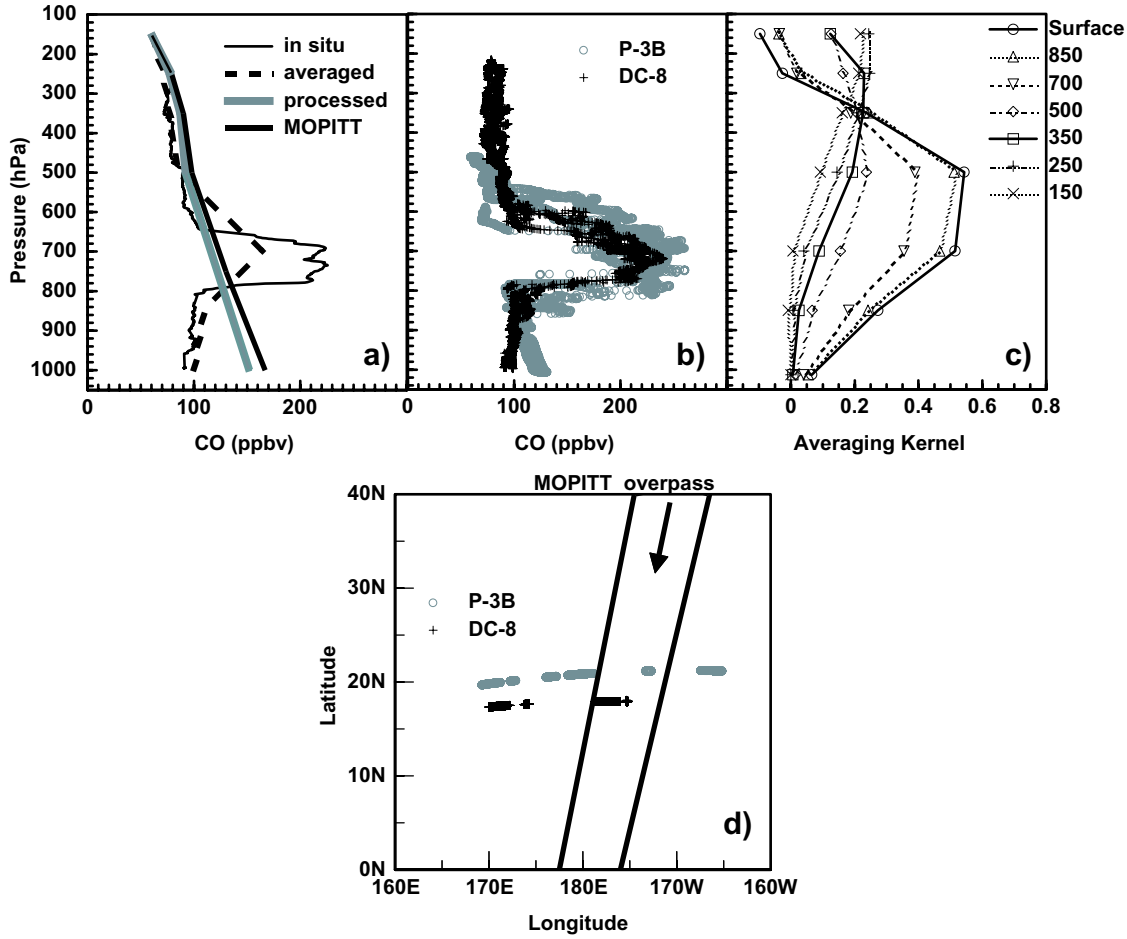

Figure 1. (a) Results from a MOPITT validation profile conducted by the NASA DC-8 on 27 February 2001. In situ data have been averaged to the MOPITT vertical resolution and processed using the MOPITT averaging kernel to allow for direct comparison. (b) Vertical distribution of CO data collected on 27 February 2001 from the NASA DC-8 and P-3 B aircraft. Data consist of 10 individual soundings between 170°E and 165°W. (c) Averaging kernel for the MOPITT retrieval in Figure 1a. Each curve describes the sensitivity of retrieved CO at a particular pressure level to perturbations to the a priori profile at different pressures. (d) Geographic distribution of samples between 600 and 800 hPa associated with the layer of enhanced CO mixing ratios and their proximity to the MOPITT overpass.

tion. In situ CO data for that profile are presented in Figure 1a. The comparison with MOPITT is also shown. As noted above, this comparison required averaging the in situ data to the seven-level vertical resolution of MOPITT followed by application of the appropriate MOPITT averaging kernel (the "processed" data). As shown in Figure 1a, the agreement between MOPITT and the processed in situ data is within 10% at all altitudes with the largest difference at the surface. The averaging kernel for this particular retrieval (Figure 1c) clearly shows MOPITT's enhanced sensitivity to midtropospheric CO and insensitivity to near-surface CO. For a detailed explanation of the averaging kernel and the mathematics of the MOPITT retrieval, the reader is referred elsewhere [e.g., *Deeter et al.*, 2003; *Emmons et al.*, 2004].

[10] Figure 1b shows the vertical distribution of CO observed from both aircraft between longitudes of 170°E and 165°W. These data encompass 10 soundings: 6 by the P-3B from near surface to ~470 hPa (6 km) and 4 by the DC-8 from near surface to ~225 hPa (11 km). The in situ soundings reveal a persistent polluted layer located between approximately 600 and 800 hPa. The sharp transition in CO at 800 hPa coincides with the trade wind inversion capping the top of the marine boundary layer. The temperature contrast across the inversion was of 4–6°C (not shown). There was also a sharp gradient in water vapor, with order of magnitude changes observed between the dry polluted layer (~500–1000 ppmv H_2O) and the wetter conditions only 20–25 hPa below the bottom of the layer.

[11] Figure 1d shows the geographic distribution of the samples taken within this polluted layer and their proximity to the MOPITT overpass. Observations covered 25° longitudinally (~2500 km) and ~4° latitudinally (~400 km). Trajectories from the aircraft sampling locations indicate that this layer originated from the Asian Pacific Rim between 30°N and 40°N latitude ~4 days earlier. Following rapid transport to the central Pacific, the polluted air mass became somewhat stagnant, spending the next 3 days

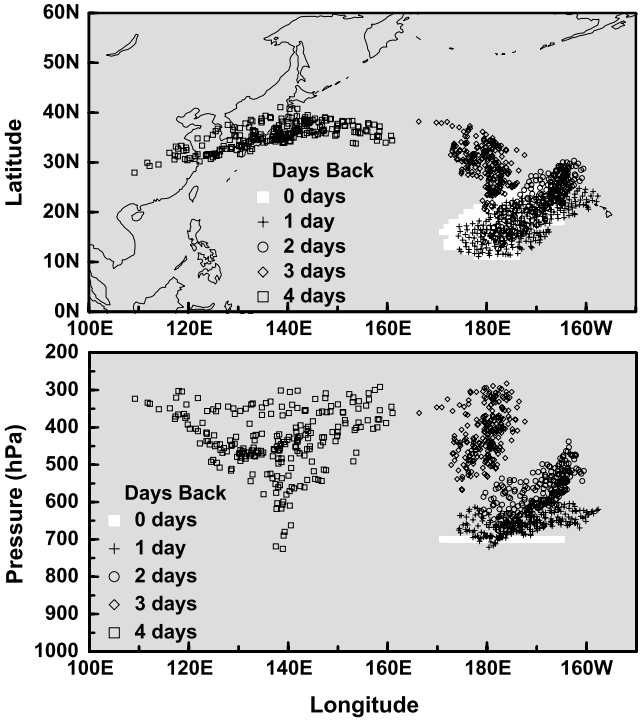

Figure 2. Transport history for an ensemble of trajectories with a common Asian Pacific Rim origin. Trajectories were isolated from a larger set of back trajectories initialized at 700 hPa between 10–25°N and 162°E–165°W. These trajectories approximate the spatial extent of the polluted layer which had been subsiding over the central North Pacific for 3 days.

subsiding and drifting southward over the central North Pacific. Given the size of the air mass and its stagnant behavior, taking a closer look at this feature through multiple MOPITT overpasses would be informative. The ability to track such a feature through satellite observations would make an important contribution to understanding the fate of Asian emissions and their impact on the global atmosphere.

4. Approach

[12] While the aircraft data indicate a polluted layer of broad geographic coverage, its full extent cannot be deduced from in situ observations alone. However, an estimate of its extent has been derived for this study based on an analysis of back trajectories. These trajectories provide a bridge between the in situ observations and the MOPITT overpasses.

[13] A cluster of back trajectories was calculated between 10–25°N and 162°E–165°W with 1° × 1° resolution. This area was deliberately chosen to be large enough to ensure that all trajectories associated with the polluted layer could be isolated. Back trajectories were initialized at 0000 UT, 28 February 2001, which was the center of the temporal window of the aircraft observations in Figure 1b. Back trajectories were initialized from the center of the polluted layer (700 hPa) as well as near the upper and lower boundaries of the layer (615 and 800 hPa). The trajectories initialized at 700 hPa are the primary trajectories used to trace the movement of the polluted layer. As discussed in section 5.2, trajectories at 615 and 800 hPa are used to estimate changes in the thickness of the polluted layer.

[14] The trajectory calculations utilized the global gridded meteorological analyses prepared by the European Centre for Medium-Range Weather Forecasts (ECMWF) [*Bengtsson*, 1985; *Hollingsworth et al.*, 1986; *ECMWF*, 1995]. The ECMWF analyses were available four times daily (0000, 0600, 1200, and 1800 UTC) at 60 vertical levels with a T319 spherical harmonic triangular truncation, interpolated to a 1° × 1° latitude-longitude horizontal grid. Back trajectories were calculated using a kinematic model employing u, v, and w wind components from the ECMWF analyses. Additional details about the trajectory model are given by *Fuelberg et al.* [1996, 1999, 2000]. Limitations of trajectories have been discussed by *Stohl* [1998], *Fuelberg et al.* [2000], and *Maloney et al.* [2001]. For these particular trajectories, their uncertainty most likely is dominated by their location in a remote, data-sparse region. The meteorological setting suggests that errors due to subscale processes (e.g., deep convection) are minimal given the slow subsidence of air during the recent history of the trajectories.

[15] The overall trajectory cluster was filtered to isolate the subset exhibiting a common origin from the Asian Pacific Rim. Figure 2 shows the behavior and extent of the polluted layer as inferred from the filtered subset of trajectories. These trajectories clearly show the stagnation and subsidence of the polluted air mass over the 3 days prior to sampling by the aircraft. They also suggest that the polluted layer had a latitudinal extent well beyond that which could be determined from the aircraft data alone. The longitudinal extent agrees well with the observations, with the exception of the far western end of the aircraft sampling (i.e., in the vicinity of 20°N, 170°E). Trajectories from this area take a somewhat different pathway back to the Asian Pacific Rim than the filtered data. This may represent some uncertainty in the exact placement of the polluted air mass as diagnosed by the trajectories. While individual trajectory errors can be quite large, the overall uncertainty in tracking the air mass is mitigated by its size and the number of trajectories exhibiting similar behavior. Fortunately, overlaps between the filtered trajectories and the MOPITT overpasses do not occur near the western edge of the feature.

[16] In section 5, the overlap between back trajectories and several MOPITT overpasses is examined. Overlap between MOPITT and the trajectories was defined by identifying those MOPITT pixels (22 × 22 km) and trajectories (1° × 1°) within a proximity of ±0.5° in both latitude and longitude.

5. Results and Analysis

[17] Figure 3 offers a qualitative assessment of the correspondence between the MOPITT CO column observations and the polluted layer as determined through back trajectories. In all cases, there is a general enhancement in MOPITT CO column for the region of overlap with trajectories. Lower values of CO column are observed both north and south of the overlap in each case. This behavior gives confidence that there is a signal in the MOPITT data that is associated with the polluted layer observed by the aircraft

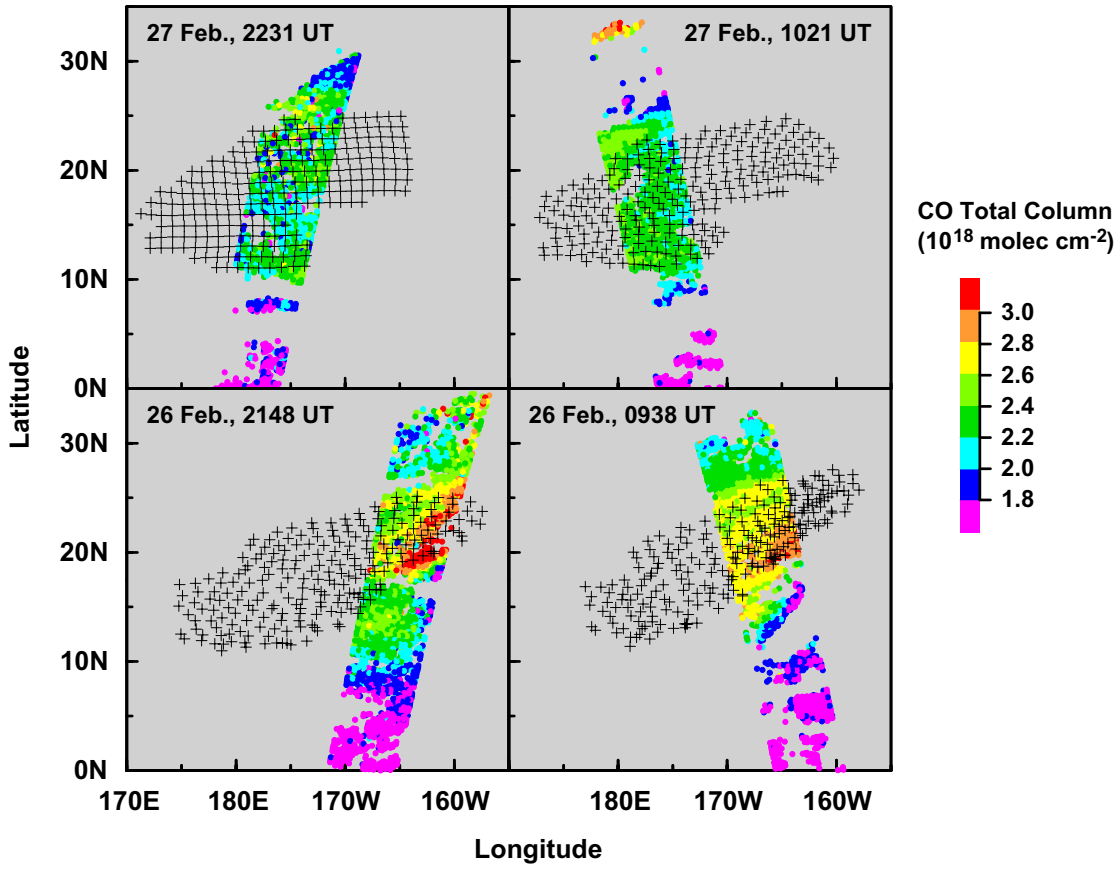

Figure 3. Overlap between the ensemble of trajectories and MOPITT for four consecutive overpasses.

and that this signal can be tracked back in time for several satellite overpasses. An interesting feature of the correspondence is that CO column amounts appear to intensify for earlier overpasses. This intensification is quantified by the statistics in Table 1. The difference between average MOPITT CO column at the time of the TRACE-P flights on 27 February (2.27×10^{18} molecules cm^{-2}) and 36 hours earlier on 26 February (2.75×10^{18} molecules cm^{-2}) represents an increase of 21%. Understanding this change in CO column associated with the polluted layer requires an examination of several factors. These factors include the impacts of dilution and chemistry, the changes in the thickness of the polluted layer, and the sensitivity of the MOPITT retrieval to the vertical distribution of CO.

5.1. Chemistry and Dilution

[18] Chemistry and dilution are expected to have little influence on the observed changes in CO column. The average CO lifetime within the enhanced layer based on box model calculations is estimated to be 45 days (diurnal average OH is 1.2×10^6 molecules cm^{-3}). Given that lifetime, the loss of CO over the 36 hours between overpasses is only 3%. Calculated CO formation due to the oxidation of methane and other hydrocarbons is expected to increase CO by ~0.5%, leading to a net loss of only 2.5%. Calculations indicate a somewhat faster loss for CO below the polluted layer and a slower loss above; however, these differences offset each other such that the 2.5% estimate for the change in CO within the polluted layer is also a reasonable estimate of the expected change in total CO column. Long-term observations of CO by *Novelli et al.* [1998] suggest that typical changes in background CO for the Northern Hemisphere are even smaller (<1% per day).

[19] Although contributions from dilution cannot be entirely eliminated from consideration, several observations suggest that dilution played a minor role in the observed changes in CO column over the 36 hours shown in Figure 3. First, CO values in the polluted layer are equivalent to

Table 1. Statistics for MOPITT CO Column and Trajectories in the Overlap Region

Overpass Date/Time	Average CO Column in Overlap, 10^{18} molecules cm^{-2}	Average Pressure Level of Trajectories in Overlap, hPa	Average Thickness of CO Layer in Overlap,[a] hPa
27 Feb., 2231 UT	2.27 ± 0.18	700 ± 2	190 ± 4
27 Feb., 1021 UT	2.32 ± 0.10	685 ± 15	193 ± 32
26 Feb., 2148 UT	2.71 ± 0.30	628 ± 24	252 ± 44
26 Feb., 0938 UT	2.75 ± 0.15	588 ± 36	282 ± 33

[a]On the basis of the average difference between trajectories initiated at 800 and 615 hPa.

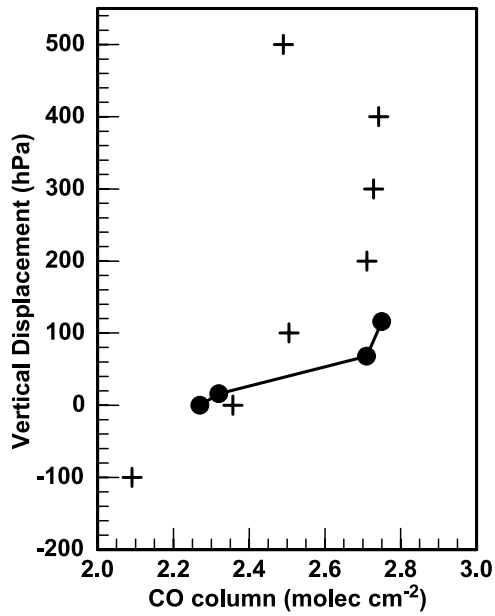

Figure 4. Calculated (crosses) and observed (circles) changes in MOPITT total CO column based on changes in the vertical location of the polluted layer. The calculated changes represent differences in retrieved column caused by moving the polluted layer upward and downward through the troposphere in 100 hPa increments from 700 hPa where the layer was sampled. The observed changes are based on the average MOPITT CO column and average pressure level of the trajectories in the overlap region (see Table 1).

median values observed in the marine boundary layer along the Asian Pacific Rim during TRACE-P and exceed the 75th percentile for Pacific Rim observations at 2–4 km. Thus the CO concentrations in the layer remain comparable to values observed near the source. Given the meteorological setting of subsidence under the high-pressure region, there is little expectation of strong vertical mixing. This is supported by the rather steep vertical gradient in CO between the plume and background CO both above and below the polluted layer. Horizontal mixing also would be limited by the sheer extent of the feature since the mixing would be limited to the edges of the polluted air mass. Finally, a polluted layer observed in the upper troposphere during the DC-8 flight of the previous day was found to have a common origin with the polluted layer analyzed here [*Heald et al.*, 2003]. Heald et al. note that trajectory analysis shows that the polluted air mass separated into two branches; one subsided over the central Pacific, and the other continued to be transported eastward in the upper troposphere over the Pacific. A comparison of these two branches by Heald et al. revealed similar chemical signatures and equivalent enhancements in both CO and total NO_y, suggesting that these branches had experienced minimal dilution over this short time period.

5.2. Thickness of the Polluted Layer

[20] The trajectories in Figure 2 exhibit gradual descent during the 3 days prior to sampling by the NASA aircraft. As noted earlier, this sinking motion was arrested by the presence of the trade wind inversion which marks the lower boundary of the polluted layer. As the descending air mass encountered this inversion, it likely experienced some degree of flattening and horizontal spreading under continued high pressure. This produced the rather broad but vertically compact layer of pollution that was observed. Thus, earlier in time, the polluted layer likely had a greater thickness which would lead to greater total CO column, albeit over a smaller area.

[21] Results for trajectories initiated at 615 and 800 hPa support the idea that the difference in detected CO column is at least partially explained by changes in the thickness of the polluted layer between overpasses. On the basis of the pressure difference between these two sets of trajectories, the statistics in Table 1 show the layer to be ~1.5 times thicker (282 versus 190 hPa) on 26 February (0938 UT) than when it was ultimately sampled by the TRACE-P aircraft 36 hours later on 27 February (2231 UT). An independent estimate of layer thickness using only the trajectories initiated at 700 hPa can be derived based on the number of trajectories versus MOPITT pixels in the overlap. For the 27 February (2231 UT) overpass, 98 trajectories overlapped with 1091 pixels (11.1 pixels/trajectory), and for the 26 February (0938 UT) overpass, 84 trajectories overlapped with 622 pixels (7.4 pixels per trajectory). The reduction in pixel/trajectory density indicates a 1/3 reduction in geographic (horizontal) coverage which would be consistent with a 50% increase in layer thickness.

[22] Changes to total CO column amount due to a change in the thickness of the polluted layer depend on the contribution of the pollution enhancement to the total column amount. On the basis of the in situ data, the pollution enhancement contributes roughly 20% to the column total. However, a more appropriate assessment comes from applying the MOPITT averaging kernel to the in situ profile as it was sampled and with the pollution enhancement removed. This results in CO column amounts of 2.36×10^{18} and 2.00×10^{18} molecules cm^{-2}; thus the pollution enhancement contributes 18% to the column amount as detected by MOPITT. On the basis of the 18% contribution to total CO column and the 50% increase in layer thickness, changes in layer thickness would be sufficient to explain a 9% (±3% given the uncertainty in the thickness) change in average CO column detected by MOPITT.

5.3. Sensitivity of the MOPITT Retrieval to the Vertical Distribution of CO

[23] In addition to changes in layer thickness, changes in the altitude of the polluted layer are also expected to affect the CO column amount detected by MOPITT, based on the vertical sensitivity of the averaging kernel. This issue has been explored by applying the MOPITT averaging kernel to the in situ profile of Figure 1a with the polluted layer displaced upward and downward by 100 hPa increments. The results of this sensitivity analysis are shown by the crosses in Figure 4. Note that the actual in situ CO column amount is unchanged; thus the changes in MOPITT retrieved CO column do not represent a change in the real column amount but only a change in the detected column based on applying the averaging kernel to different vertical distributions of CO. The change in retrieved CO column

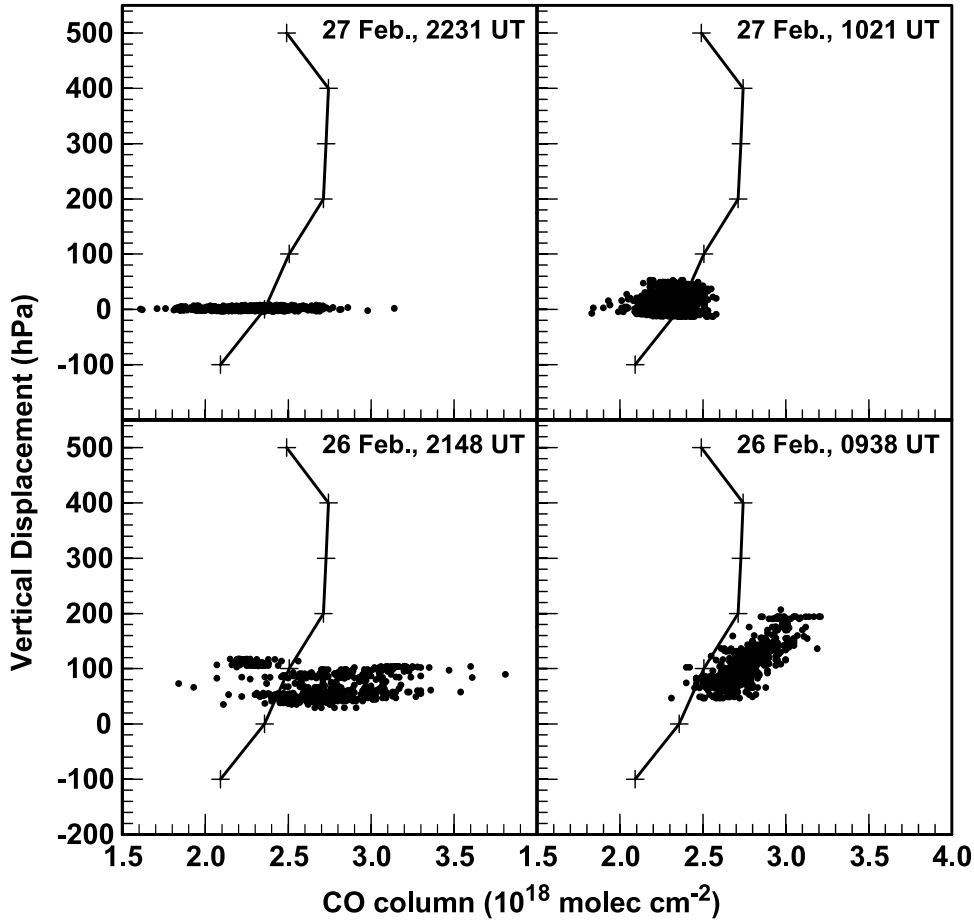

Figure 5. Same as Figure 4 except individual MOPITT observations are shown for each MOPITT overpass instead of average conditions within the overlap. Vertical displacement of a given MOPITT observation is based on the nearest trajectory.

ranges from a low value of 2.09×10^{18} molecules cm^{-2} for a displacement of -100 hPa to a high of 2.74×10^{18} molecules cm^{-2} for a displacement of +400 hPa.

[24] Average MOPITT CO column and vertical displacement for the overlap between MOPITT and the trajectories initiated at 700 hPa are also shown in Figure 4 (also see numbers in Table 1). While the trajectory-derived change in altitude over the 36 hour period between overpasses is just over 100 hPa, this change occurs at pressures where MOPITT is quite sensitive to vertical displacement of the layer. On the basis of the retrieval sensitivity (see crosses in Figure 4), changes in the altitude of the polluted layer contributes ~7% (±3% given the uncertainty in average pressure level) to the retrieved change in average CO column observed over the 36 hour period.

[25] The effects of changes in the altitude of the polluted layer are further examined in Figure 5. Here all individual MOPITT observations within the overlap are shown along with the estimated vertical displacement based on the nearest trajectory. One initial observation is that the range of observed MOPITT values is much greater under daylight conditions (note that since observations were made near the international dateline, data for 2231 UT, 27 February, and 2148 UT, 26 February, represent daylight conditions). This greater variability is also reflected in the standard deviations for CO column reported in Table 1. These numbers indicate that daylight data exhibit approximately twice the variability of data collected at night.

[26] There is a strong relationship between vertical displacement and CO column for the nighttime data on 26 February (0938 UT). The lack of a relationship for data from previous overpasses should be acknowledged; however, this may be due to the greater variability for the daytime data and the smaller range of vertical displacement in prior overpasses. The data for 26 February (0938 UT) exhibit displacements of as much as 200 hPa and show a strong correlation between CO column and displacement (R^2 = 0.63). This correlation between CO column and displacement provides additional confidence that the sensitivity of MOPITT observations to changes in the vertical distribution of CO is consistent with expectations. As discussed in section 5.2, the systematic shift in the data toward larger CO columns can be explained by the increased thickness of the polluted layer on 26 February (0938 UT).

5.4. Day-Night Variability

[27] The differences between daylight and nighttime MOPITT data seen in Figure 5 merit further discussion. Discussion of day/night influence on MOPITT retrievals is

Table 2. MOPITT CO Column Statistics Versus Cloud Flag

	Daylight Conditions 27 February, 2231 UT		Dark Conditions 27 February, 1021 UT	
Cloud Flag	Percent Data	CO ± SD	Percent Data	CO ± SD
1	1	2.41 ± 0.20	5	2.28 ± 0.11
2	40	2.27 ± 0.17	13	2.30 ± 0.10
3	3	2.16 ± 0.35	no data	no data
4	56	2.28 ± 0.17	82	2.32 ± 0.10
	Daylight Conditions 26 February, 2148 UT		Dark Conditions 26 February, 0938 UT	
Cloud Flag	Percent Data	CO ± SD	Percent Data	CO ± SD
1	2	2.45 ± 0.28	20	2.66 ± 0.10
2	46	2.68 ± 0.28	6	2.66 ± 0.12
3	4	2.76 ± 0.39	1	2.65 ± 0.12
4	48	2.75 ± 0.30	73	2.78 ± 0.15

typically reserved for observations over land where there are large day/night differences in surface conditions [*Deeter et al.*, 2002, 2003]. Observations are expected to be least sensitive to this effect over tropical ocean regions where diurnal variability in surface conditions is small [*Deeter et al.*, 2002]; however, these results show that day/night differences are nontrivial even for this region. It is likely that the increased variability in CO during the day is related to the retrieval of the surface emissivity, which is performed simultaneously with the retrieval of CO mixing ratios [*Deeter et al.*, 2003]. MOPITT's thermal band radiances are more sensitive to surface emissivity at night than during the day, and consequently less sensitive to the CO distribution at night. Therefore the CO retrieval errors are larger at night than during the day, resulting in greater reliance on the CO a priori profile. The nighttime CO retrieval will thus be closer to the a priori profile and show less variability than the daytime CO. Indeed, average reported errors are larger at night (9–10%) than during the day (6–7%) reflecting a larger a priori influence in the nighttime data.

[28] Differences in cloud detection for daylight and dark conditions were also examined as a potential contributor to the day/night difference in variability. The presence of clouds in MOPITT pixels is determined using both MOPITT temperature retrievals and the Moderate Resolution Imaging Spectroradiometer (MODIS) cloud mask product (details are available at http://www.eos.ucar.edu/mopitt/data/index.html; Retrieval Information). An important benefit of incorporating the MODIS cloud mask is the ability to identify low cloud. Retrievals over low cloud are possible since MOPITT is insensitive to the lowest portion of the atmosphere. MOPITT's flag for cloud description allows for 16 different possibilities, but only 4 occur for the data examined here: (1) clear, only MOPITT thermal used, (2) MOPITT and MODIS cloud mask agree on clear, (3) MODIS cloud mask only clear (when MOPITT determines cloudy), and (4) MOPITT overriding MODIS cloud mask over low clouds (MODIS test flags used).

[29] Table 2 gives MOPITT CO column statistics for the various cloud flags under daylight and dark conditions. While there is a difference in the distribution of cloud flags between daylight and dark, these cloud flags do not appear to have a significant influence on average statistics for MOPITT CO column. Under dark conditions, the dominant condition is a cloud flag of 4 (>70% of data). For daylight conditions, the data are more evenly split between cloud flags of 2 and 4. The similarity in CO statistics under daylight conditions for cloud flags 2 and 4 show that the MOPITT strategy of using MODIS to discriminate for low cloud is effective.

6. Discussion and Implications

[30] The most encouraging result of this analysis is that the behavior of the MOPITT data is consistent with expectations. From the statistics in Table 1, the average CO column for 26 February (0938 UT) is increased over that of 27 February (2231 UT) by a ratio of 1.21. The majority of this difference is consistent with two effects: the change in layer thickness (9%) and the change in MOPITT sensitivity to the altitude of the layer (7%). The product of these two differences yields a ratio of 1.17 which would account for 80% of the observed change in average CO column. Adding the estimated impact of chemistry (2.5%) brings the estimate to within 10% of the observed change. While not conclusive, this level of closure lends confidence to the idea that the major factors contributing to the observed change in CO column have been identified.

[31] The results of this analysis are beneficial in several ways: (1) they contribute to a better understanding of the sources of variability in satellite observations, (2) they provide the basis for exploring alternative strategies for validation and in situ sampling in support of satellite observations, and (3) they demonstrate the link between satellite observations and the detailed process studies pursued by research aircraft.

6.1. Sources of Variability

[32] Of the seven validation profiles flown during TRACE-P, only four were in skies clear enough to yield a comparison with MOPITT. The variation in MOPITT retrieved CO column for those four attempts was only 16%. The variation across the four overpasses analyzed here was 21% and could have been greater (~30% based on Figure 4) if the polluted layer had been traceable further back in time. The fact that this change was due to multiple factors (both real and artificial) highlights the importance of taking opportunities to integrate in situ and satellite data to better understand the possible sources of variation in satellite observations. The difference in day/night data also represents an important source of variability worthy of further study.

6.2. Validation and Sampling in Support of Satellites

[33] While rigorous validation requires in situ profiles coincident with observations from satellite, this analysis suggests that additional insight can be gained from a broader sampling of the surrounding region as well. It also suggests that validation profiles could benefit from a targeted approach aimed at pursuing large-scale features. For instance, additional back trajectories from the central North Pacific during the TRACE-P period (February–March 2001) indicate that emissions from the Asian Pacific Rim are transported to the central North Pacific in a manner similar to that shown in this analysis roughly once every 10 days. This transport as well as cross-Pacific

transport of Asian emissions can be reasonably predicted by global models [*Heald et al.*, 2003] and could be used as a guide to the best opportunities for taking in situ measurements in coordination with satellites. Improving the ability to observe the behavior and frequency of individual large-scale perturbations as they transport emissions from source regions to remote regions is important for understanding the incorporation of source emissions into the global atmosphere.

[34] It would also be useful for some in situ sampling in conjunction with MOPITT overpasses to be conducted at night. This would help evaluate day/night differences in MOPITT variability (see Table 1 and Figure 5).

[35] This analysis would be much more definitive if in situ data had been available for each of the four consecutive overpasses, but one must also ask whether such a goal is realistic. Certainly it would be worthwhile to test the ability of forward trajectories and global (or regional) model predictions to identify large-scale features and dictate the optimal times for conducting validation profiles. The primary complicating factor would be waiting to see whether the feature and the satellite would intersect for consecutive overpasses, the probability of which would largely depend on the size of the feature.

6.3. Linking Satellite Observations and Detailed Process Studies

[36] The polluted layer analyzed here was characterized by enhanced mixing ratios for many constituents in addition to CO. Of particular importance, ozone mixing ratios in excess of 80 ppbv were encountered in the layer, representing values well above those observed in air closer to the Asian Pacific Rim during TRACE-P. Understanding the photochemical evolution of this air mass as it relates to ozone production, the interconversion of reactive nitrogen species, and the oxidation chemistry of a pollution plume are central to the goals of the TRACE-P mission. Although beyond the scope of this paper, the chemical evolution of this polluted layer has been investigated in detail using a three-dimensional model [*Heald et al.*, 2003] and Lagrangian trajectory modeling (A. Hamlin, manuscript in preparation, 2004).

[37] It is expected that this polluted plume does not represent an isolated incident. It more likely represents an episodic transport pathway for emissions from the Asian Pacific Rim. The extent to which this particular transport pathway can be diagnosed from MOPITT observations is highlighted by this analysis. Given the additional details provided by the full suite of TRACE-P measurements, further attempts to diagnose the frequency and magnitude of similar transport events using MOPITT data would be useful not just for understanding CO. Some expectation of the impact on other species could be made by inference from the TRACE-P aircraft data.

7. Conclusion

[38] Airborne sampling over the central North Pacific during TRACE-P revealed a polluted layer characterized by enhanced CO mixing ratios between 600 and 800 hPa that were more than double background values for the rest of the column. Sampling of this layer included a vertical profile conducted in coincidence with an overpass of the MOPITT instrument onboard the EOS Terra satellite. This profile, along with sampling over the surrounding area by NASA's DC-8 and P-3B aircraft revealed that the layer covered a geographic range of at least 25° longitude (~2500 km) and 4° latitude (~400 km).

[39] The full geographic extent of the layer was estimated using back trajectory analysis. The layer then was tracked back in time to examine the overlap between the feature and MOPITT observations for four consecutive overpasses. The MOPITT data for these four overpasses showed clear signs of enhanced CO column associated with the position of the layer as diagnosed by trajectories. Enhancements in MOPITT CO column and the trajectories agreed well. However, the average CO column associated with the trajectories increased by 21% back in time across the 36 hours covered by the four overpasses. Several possible reasons for the change in average CO column were investigated. These included chemistry, dilution, change in the thickness of the layer, and the sensitivity of the MOPITT retrieval to the altitude of the layer.

[40] Results of this analysis suggest that most of the change in average CO column is consistent with a physical change in the thickness of the layer (9%) and changes in the retrieved column amount due to the altitude of the layer (7%). Changes due to chemistry were estimated to be much smaller (2.5%), and the impact of dilution, while difficult to quantify, was expected to be even smaller. Taken together, these impacts can account for 90% of the observed change in MOPITT CO column.

[41] An examination of the altitude of individual trajectories versus MOPITT CO column revealed a good correlation (R^2 = 0.62) and a trend similar to that expected based on the sensitivity of the MOPITT retrieval to the altitude of the layer. This exercise also revealed greater variability in CO column for daytime versus nighttime observations.

[42] These results provide insight on the sources of variability (both real and artificial) in satellite observations. Understanding these sources of variability is important if MOPITT observations are to be quantitatively useful. This analysis also suggests that validation strategies might benefit from broader regional sampling in support of validation profiles as well as preplanned targeting of large-scale features. This also would facilitate the evaluation of forward trajectories and global/regional models used to forecast the presence and timing of pollution transport. The importance of the link between aircraft and satellite data is demonstrated here in the wealth of detail that in situ observations provide versus the long-term tracking of transport through satellite observations. While the airborne data provide the opportunity for a detailed examination of the chemical evolution of transport from the Asian Pacific Rim to the central North Pacific, satellite observations from MOPITT offer the possibility of monitoring the frequency and strength of such transport events.

[43] **Acknowledgments.** This work was supported by the NASA Tropospheric Chemistry Program. C.L.H. was supported by the Natural Science and Engineering Research Council of Canada and NASA Headquarters under Earth System Science Fellowship grant NGT5-30466. The

authors would like to thank the pilots and crew of NASA's DC-8 and P-3B aircraft for their efforts in support of the TRACE-P flights.

References

Bengtsson, L. (1985), Medium-range forecasting—The experience of ECMWF, *Bull. Am. Meteorol. Soc.*, *66*, 1133–1146.

Deeter, M. N., G. L. Francis, D. P. Edwards, J. C. Gille, E. McKernan, and J. R. Drummond (2002), Operational validation of the MOPITT instrument optical filters, *J. Atmos. Oceanic Technol.*, *19*, 1772–1782.

Deeter, M. N., et al. (2003), Operational carbon monoxide retrieval algorithm and selected results for the MOPITT instrument, *J. Geophys. Res.*, *108*(D14), 4399, doi:10.1029/2002JD003186.

Drummond, J. R., and G. S. Mand (1996), The Measurements of Pollution in the Troposphere (MOPITT) instrument: Overall performance and calibration requirements, *J. Atmos. Oceanic Technol.*, *13*, 314–320.

Eisele, F. L., et al. (2003), Summary of measurement intercomparisons during TRACE-P, *J. Geophys. Res.*, *108*(D20), 8791, doi:10.1029/2002JD003167.

Emmons, L. K., et al. (2004), Validation of Measurements of Pollution in the Troposphere (MOPITT) CO retrievals with aircraft in situ profiles, *J. Geophys. Res.*, *109*, D03309, doi:10.1029/2003JD004101.

European Centre for Medium-Range Weather Forecasts (ECMWF) (1995), User guide to ECMWF products 2.1, *Meteorol. Bull., M3.2*, Reading U.K.

Fishman, J., C. E. Watson, J. C. Larsen, and J. A. Logan (1990), Distribution of tropospheric ozone determined from satellite data, *J. Geophys. Res.*, *95*, 3599–3617.

Fishman, J., J. M. Hoell Jr., R. D. Bendura, R. J. McNeal, and V. W. J. H. Kirchoff (1996), NASA GTE TRACE A experiment (September–October 1992), Overview, *J. Geophys. Res.*, *101*, 23,865–23,879.

Fuelberg, H. E., R. O. Loring Jr., M. V. Watson, M. C. Sinha, K. E. Pickering, A. M. Thompson, G. W. Sachse, D. R. Blake, and M. R. Schoeberl (1996), TRACE-A trajectory imtercomparison: 2. Isentropic and kinematic methods, *J. Geophys. Res.*, *101*, 23,927–23,939.

Fuelberg, H. E., R. E. Newell, S. P. Longmore, W. Zhu, D. J. Westberg, E. V. Browell, D. R. Blake, G. L. Gregory, and G. W. Sachse (1999), A meteorological overview of the PEM-Tropics period, *J. Geophys. Res.*, *104*, 5585–5622.

Fuelberg, H. E., J. R. Hannan, P. F. J. van Velthoven, E. V. Browell, G. Bieberbach Jr., R. D. Knabb, G. L. Gregory, K. E. Pickering, and H. B. Selkirk (2000), A meteorological overview of the SONEX period, *J. Geophys. Res.*, *105*, 3633–3651.

Heald, C. L., et al. (2003), Asian outflow and trans-Pacific transport of carbon monoxide and ozone pollution: An integrated satellite, aircraft, and model perspective, *J. Geophys. Res.*, *108*(D24), 4804, doi:10.1029/2003JD003507.

Hollingsworth, A., D. B. Shaw, P. Lonnberg, L. Illari, K. Arpe, and A. J. Simmons (1986), Monitoring of observations and analysis quality by a data assimilation system, *Mon. Weather Rev.*, *114*, 861–879.

Jacob, D. J., J. H. Crawford, M. M. Kleb, V. S. Connors, R. J. Bendura, J. L. Raper, G. W. Sachse, J. C. Gille, L. Emmons, and C. L. Heald (2003), The Transport and Chemical Evolution over the Pacific (TRACE-P) mission: Design, execution and overview of results, *J. Geophys. Res.*, *108*(D20), 9000, doi:10.1029/2002JD003276.

Maloney, J. C., H. E. Fuelberg, M. A. Avery, J. H. Crawford, D. R. Blake, B. G. Heikes, G. W. Sachse, S. T. Sandholm, H. Singh, and R. W. Talbot (2001), Chemical characteristics of air from different source regions during the second Pacific Exploratory Mission in the Tropics (PEM-Tropics B), *J. Geophys. Res.*, *106*, 32,609–32,625.

Novelli, P. C., K. A. Masarie, and P. M. Lang (1998), Distributions and recent changes of carbon monoxide in the lower troposphere, *J. Geophys. Res.*, *103*, 19,015–19,033.

Sachse, G. W., G. F. Hill, L. O. Wade, and M. G. Perry (1987), Fast-response, high-precision carbon monoxide sensor using a tunable diode laser absorption technique, *J. Geophys. Res.*, *92*, 2071–2081.

Singh, H. B., and D. J. Jacob (2000), Future directions: Satellite observations of tropospheric chemistry, *Atmos. Environ.*, *34*, 4399–4401.

Stohl, A. (1998), Computation, accuracy, and application of trajectories-A review and bibliography, *Atmos. Environ.*, *32*, 947–966.

Vay, S. A., et al. (1998), DC-8–based observations of aircraft CO, CH_4, N_2O, and $H_2O_{(g)}$ emission indices during SUCCESS, *Geophys. Res. Lett.*, *25*, 1717–1720.

G. Chen, J. H. Crawford, and V. S. Connors, Atmospheric Sciences, NASA Langley Research Center, Mail Stop 483, Hampton, VA 23681-0001, USA. (g.chen@larc.nasa.gov; james.h.crawford@nasa.gov; vickie@stormy.larc.nasa.gov)

M. N. Deeter, D. P. Edward, L. K. Emmons, and J. C. Gille, National Center for Atmospheric Research, 1850 Table Mesa Drive, Boulder, CO 80307, USA. (mnd@ucar.edu; edward@uars1.acd.ucar.edu; emmons@ucar.edu; gille@ncar.ucar.edu)

H. E. Fuelberg and D. M. Morse, Department of Meteorology, Florida State University, 404 Love Building, Tallahassee, FL 32306-4520, USA. (fuelberg@met.fsu.edu)

A. J. Hamlin, Department of Engineering Fundamentals, Michigan Technological University, 870 Dow Environmental Sciences and Engineering Bldg., 1400 Townsend Drive, Houghton, MI 49931, USA. (reh@mtu.edu)

C. L. Heald, Department of Earth and Planetary Sciences, Harvard University, 29 Oxford Street, Cambridge, MA 02138, USA. (heald@fas.harvard.edu)

C. Kittaka and J. R. Olson, NASA Langley Research Center, Mail Stop 410B, Hampton, VA 23681, USA. (c.kittaka@larc.nasa.gov; j.r.olson@larc.nasa.gov)

G. W. Sachse, NASA Langley Research Center, Mail Stop 472, Hampton, VA 23681, USA. (g.w.sachse@larc.nasa.gov)